Gene Expression within the Amacrine Cell Layer of Chicks after Myopic and Hyperopic Defocus

Regan Scott Ashby and Marita Pauline Feldkaemper

Purpose. Ocular growth is regulated locally by signals produced in the retina. The highly heterogeneous nature of the retina may mask important changes in gene expression during global analysis. This study was conducted to investigate changes in gene expression specifically within the amacrine cell layer (ACL), the most likely generator of growth signals, during optical manipulation of ocular growth.

Method. Chicks were monocularly treated with either −7-D (n = 6) or +7-D (n = 6) lenses for 24 hours. Untreated age-matched chicks served as control subjects (n = 6). Total RNA from the ACL was isolated from 10-μm-thick sections, obtained using laser capture microdissection. Labeled cRNA was prepared from three samples per condition and hybridized to chicken genome microarrays. Changes in gene expression were validated by using semiquantitative real-time RT-PCR.

Results. One hundred twenty-eight genes were differentially expressed in the ACL of the minus lens–treated eyes, whereas the plus lens–treated eyes displayed 58 changes 24 hours after treatment. Only 11 genes were differentially expressed under both experimental conditions, whereas the expression of only one gene (clone *ChEST927g14*) was modulated by the sign of defocus. Compared with previous studies in the field, the magnitude of changes observed in the present work were larger, with more than 30% of differentially expressed genes showing a twofold or greater modulation in expression. The results, obtained from independent validation by real-time RT-PCR technology, correlated highly with the original microarray data. The differential expression of four of eight genes was validated in plus lens–treated eyes, and eight of nine genes were independently validated in minus lens–treated eyes.

Conclusions. The targeted investigation of the ACL enabled the identification of several novel genes that may form part of the growth regulatory pathways of the eye. Different retinal pathways may underlie the response of the eyes to plus and minus lens compensation, as there was limited overlap in the regulated genes observed within the ACL under both conditions. (*Invest Ophthalmol Vis Sci.* 2010;51:3726–3735) DOI:10.1167/iovs.09-4615

Myopia is an ocular disorder brought about by a mismatch between the axial length of the eye and its optical properties. This mismatch causes the focal plane of distant objects to fall in front of the retina when the eye is at rest, instead of on it, causing the images to appear blurred. In most cases, myopia is the result of excessive elongation of the eye, rather than alterations in the optical properties of either the cornea or lens. Myopia has emerged as a major epidemic in many parts of the world, most notably in urban East Asia, with a prevalence in those finishing secondary or high school ~80% to 90% and ~20% having high myopia (< −6 D),[1] leading to an increased risk of chorioretinal degeneration.[2]

Research into possible optical and pharmacologic treatments for prevention of myopia, and particularly high myopia, has been aided by the discovery that the rate of eye growth can be manipulated experimentally in animal models by altering their visual experience through the deprivation of form vision or the fitting of spectacle lenses in front of the eye.[3,4] The fitting of minus lenses over the eye pushes the image plane behind the retina, causing hyperopic defocus.[4] This effect induces an increase in the rate of ocular growth, through rapid thinning of the choroid[5] and the slower process of increased scleral growth,[6] allowing the retina to be moved toward the correct focal plane. In contrast, the fitting of plus lenses in front of the eye causes the image plane to fall in front of the retina, producing myopic defocus. The eye compensates for the imposed defocus by pushing the retina forward toward the new focal plane through rapid swelling of the choroid and, more slowly, a reduction in the rate of scleral growth.[5]

The pathways and molecules involved in the regulation of ocular growth are still unclear. Animal studies have demonstrated that eye growth is actively regulated, in response to visual stimuli, by local retinal mechanisms that send signals to, or past, the RPE/choroid to control the growth of the scleral tissue. Consequently, several studies have been undertaken to investigate global changes in retinal gene and protein expression during manipulation of ocular growth, in an attempt to elucidate the biochemical pathways underlying it.[7–13] However, because of the highly heterogeneous nature of the retina, differential gene expression within subpopulations of retinal cells could mask important changes in gene and protein expression when investigated at the whole retinal level.

Retinal amacrine cells appear to be critically involved in the modulation of ocular growth. In support of this conclusion, animal studies have demonstrated that amacrine cells express and/or release numerous biochemical markers postulated to be involved in the modulation of ocular growth, including: Egr-1,[14] glucagon,[15,16] dopamine,[17,18] Pax6,[19,20] cellular retinoic acid binding protein (CRABP),[21] retinoic acid receptor (RAR),[22] cytochrome-*c* oxidase,[23] and vasoactive intestinal polypeptide (VIP).[24,25] Furthermore, key pharmacologic agents found to influence ocular growth specifically target transmitter systems expressed by the amacrine cells,[15,17,18,26–28] whereas neural toxins that alter eye growth commonly target these retinal neurons.[29–31] Therefore, we focused specifically on changes in RNA transcript levels within the amacrine cell layer (ACL) of the chick eye, a well-established model for eye growth, during visual manipulation of ocular growth. Although

From the Institute for Ophthalmic Research, Section of Neurobiology of the Eye, University of Tübingen, Tübingen, Germany.

Supported by the Marie-Curie Research Training Network MyEuropia Grant MRTN-CT-2006-034021.

Submitted for publication September 9, 2009; revised November 21, 2009, and January 17 and February 12, 2010; accepted February 20, 2010.

Disclosure: **R.S. Ashby**, None; **M.P. Feldkaemper**, None

Corresponding author: Regan Scott Ashby, Institute for Ophthalmic Research, Section of Neurobiology of the Eye, University of Tübingen, Calwerstrasse 7/1, 72076 Tübingen, Germany; regan.ashby@anu.edu.au.

most changes observed represent differential gene expression within retinal amacrine cells, this fundal layer is complex and also contains cell bodies of displaced bipolar and ganglion cells, as well as the processes of bipolar cells and Müller cells. Also, displaced amacrine cells, as well as those amacrine cells that sit deeper within the inner nuclear layer, may be missed. However, in general, the extracted sample of tissue is enriched in amacrine cell bodies.

METHODS

Animal Housing

One-day-old white leghorn chicks were obtained from a local hatchery in Kirchberg, Germany. The chicks were maintained in temperature-controlled rooms under a 12:12 hour light–dark cycle, with incandescent illumination of ~500 lux during the light phase, and <1 lux in the dark phase (lights on at 7 AM and off at 7 PM). Chickens had access to unlimited amounts of food and water and were given 5 days to become accustomed to their surroundings before the commencement of experiments. All experiments conformed to the ARVO Statement for the Use of Animals in Ophthalmic and Vision Research and were approved by the University Commission for Animal Welfare.

Experimental Treatment

The methods used for lens-induced changes in ocular growth have been published in detail.[15] Briefly, on the day before treatment, 7-day-old chicks were anesthetized with diethyl-ether and fitted with a ring (Velcro; Velcro GmbH, Freiberg am Neckar, Germany) attached around the left eye with super glue. On the following day, the chicks were split into three experimental groups: (1) minus lens–treated (n = 6), (2) plus lens–treated (n = 6), and (3) age-matched untreated control (n = 6). All animals were exposed to the treatment regimen for 24 hours beginning at 12 PM. For the lens-treated groups, either a −7- or +7-D lens was fitted to the left eye with a similar mounting system (Velcro; Velcro GmbH). After 24 hours of treatment, the chicks were killed with an overdose of diethyl ether. The left eye of each chick, including that of each age-matched untreated control animal, was removed and hemisected, with the anterior portion of the eye and vitreous body discarded. The contralateral control eyes from the chicks in each experimental group were not used in this study because of the possible cross-talk between the eyes reported in the literature. The posterior eye cup was immediately frozen in tissue-freezing medium (Leica, Nussloch, Germany) at −20°C in preparation for sectioning. Ten-micrometer-thick frozen sections were then cut on a cryostat (HM500; Microm, Walldorf, Germany) and collected on 1-mm slides (Pen Membrane; Carl Zeiss Meditec, Bernried, Germany) for laser-capture microdissection (LCM). The slides were immediately frozen at −70°C for processing the following day. The same treatment regimen was used for the analysis of whole retina samples (24 hours treatment: +7-D lens, −7-D lens, or no lens wear, n = 5 per group). Retinal punches from the left eye were prepared carefully to ensure that the samples were not contaminated with retinal pigment epithelium and then immediately snap-frozen in liquid nitrogen and stored at −70°C. RNA was extracted (RNeasy Mini Kit; Qiagen, Hilden, Germany), according to the manufacturer's instructions.

Laser Capture Microdissection

For LCM, frozen sections were allowed to thaw briefly (1 minute) before fixation in chilled (4°C) 70% ethanol for 2 minutes. The sections were briefly stained (1 minute) in 1% crystal violet for visualization of the retinal layers. The slides were then taken through a dehydration series (70%, 85%, 95%, and 100% ethanol, 1 minute per concentration), before being washed twice in xylene for 2 minutes per period, to remove any remaining alcohol. The sections were air dried in a fume hood (~3 minutes) to remove the remaining xylene, before being immediately placed on the microdissection stage for processing. A microbeam laser capture system (PALM; Carl Zeiss Meditec) was used to remove the ACL (Fig. 1) from eight sections per eye for later analysis by microarray.

Microarray Analysis

Roughly 0.3 ng of total RNA was extracted from LCM sections (RNeasy Micro Kit; Qiagen), according to the manufacturer's instructions. Microarray analysis was performed by the Affymetrix Resource Facility (University of Tübingen, Germany) on three of the six samples collected for each experimental treatment (minus lens wear, plus lens

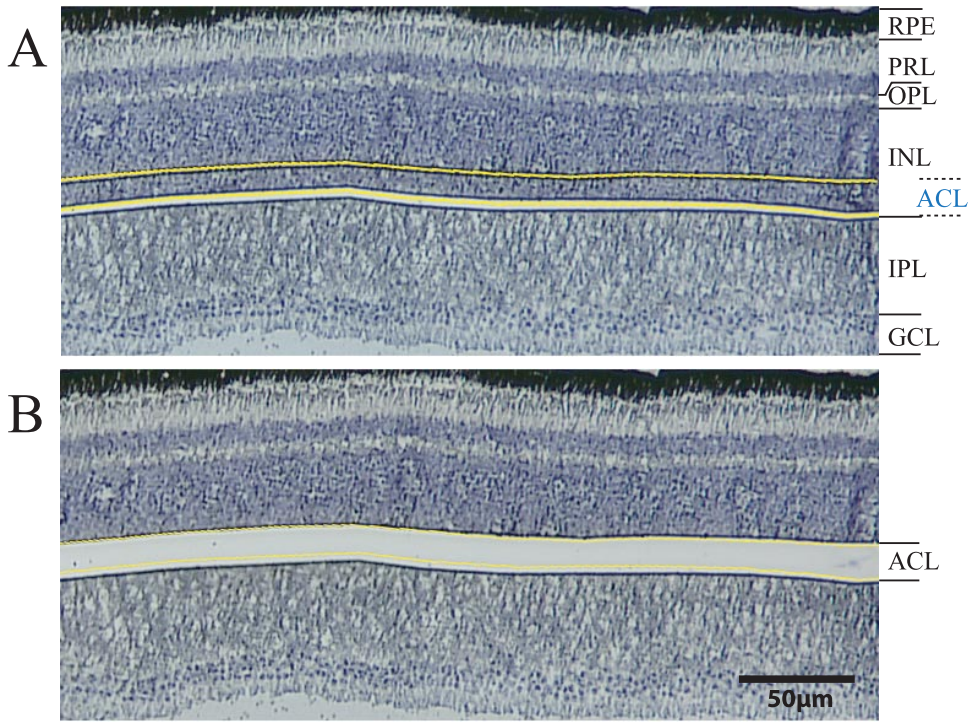

FIGURE 1. (**A**) A retinal section after LCM of the ACL. (**B**) A retinal section after catapulting and collection of the ACL. RPE, retinal pigment epithelium; PRL, photoreceptor layer; OPL, outer plexiform layer; INL, inner nuclear layer; ACL amacrine cell layer; IPL, inner plexiform layer; GCL, ganglion cell layer.

wear, and untreated control). The methods used for the preparation and analysis of samples by microarray technology (Affymetrix; Santa Clara, CA) have been described in detail.[9] In brief, RNA quality and quantity were checked (model 2100 Bioanalyzer; Agilent Technologies, Böblingen, Germany) and a nanodrop system (ND1000; PeQlab, Erlangen, Germany). Total RNA was reverse transcribed to cDNA using oligo(dT) primers containing a T7 RNA polymerase promoter. After cDNA synthesis in the first cycle, an unlabeled ribonucleotide mix was used in the first cycle of in vitro transcription amplification. The unlabeled cRNA was then reverse transcribed in the first-strand cDNA synthesis step of the second cycle using random primers. Subsequently, a T7-Oligo (dT) promoter primer was used in the second-strand cDNA synthesis to generate double-stranded cDNA template containing a T7 promoter. The resulting double-stranded cDNA was amplified and labeled with a biotinylated nucleotide analogue/ribonucleotide mix in a second in vitro transcription reaction. The labeled cRNA samples were then cleaned up, fragmented, and hybridized onto gene microarray chips (Chicken Genome Array Chips; Affymetrix), according to the manufacturer's protocol, with a coverage of 32,773 transcripts, corresponding to more than 28,000 chicken genes. Scanning and analysis of the chips was performed (Microarray Suite Software, ver. 5.0; Affymetrix) and the signal intensities analyzed (ArrayAssist 5.5.1; Stratagene, La Jolla, CA). GC RMA normalization data were corrected for multiple testing by using the Benjamini-Hochberg test with a false discovery rate of 5%. Microarray data were analyzed by using a GC-RMA normalization method, as it produces fewer false positives than Mas5 normalization, while accounting for sequence-specific probe affinities of the microarray probes to attain more accurate gene expression values than its predecessor (RMA normalization). The generated gene lists for RMA and Mas5 normalization can be found within the supplementary material, available at http://www.iovs.org/cgi/content/full/51/7/3726/DC1. All primary microarray data have been deposited in the Gene Expression Omnibus database (accession number GSE17758) (GEO; http://www.ncbi.nlm.nih.gov/geo; maintained in the public domain by The National Center for Biotechnology Information, Bethesda, MD).

Semiquantitative Real-Time RT-PCR

Fourteen genes of interest were chosen for further analysis and validation using real-time RT-PCR (Table 1). Two micrograms of total RNA was reverse transcribed to first-strand cDNA with a superscript cDNA

Table 1. Sequences and Efficiency Values for Gene Specific Primers Used in Real-Time RT-PCR

Gene No.	Gene Name	Gene Symbol	Forward Sequence	Reverse Sequence	Probe ID	Efficiency	Product Size
1	Angiopoietin	*ANGPT2*	GCACCAGATGCCTGATTGTC	CACTGAGAGCCTACTGCTTC	Gga.3259.1.S1_at	1.89	251
2	ChEST267a2	*ChEST267a2*	GCAAAGAGAAGCCAGTGGAA	CTAGGCCAGCAGCAGTGATT	Gga.10694.1.S1_at	1.88	110
3	ChEST49o10	*ChEST49o10*	GCCCTCCTGCTAAGACTGAA	GGCCAGTAAGCAAAGCAAAG	Gga.13753.1.S1_at	2.08	170
4	Cytochrome P450, family 26, subfamily A, polypeptide 1	*CYP26A1*	GCCGATCTCTTTACCGACAA	GCAGATTGTCCACAGGGTAC	Gga.331.1.S1_at	1.92	247
5	Zinc finger, DHHC-type containing 14	*DHHC14*	CATGCCACGCTACAGTATGT	CCATCTTCTAGGCACCACTG	GgaAffx.21352.1.S1_at	1.91	184
6	D4, zinc and double PHD fingers, family 3	*DPF3*	ACTGCTATGCATGGTTGCTG	TTGGGCAGTAACAACTGGTG	Gga.46.1.S1_a_at	1.93	206
7	Guanine nucleotide binding protein gamma 13	*GNG13*	TGTCCTCCAAGACGATACCC	CACTTCCCTTTCTCCACCCA	Gga.10842.1.S1_at	1.83	115
8	Glial cell line derived neurotrophic factor, family receptor alpha 1	*GFRAI*	AAGTGATTCTGCGTTCCCTG	GAGCTTTCACAATGGCTGCT	Gga.588.1.S1_at	1.89	193
9	General transcription factor IIH, polypeptide 5	*GTF2H5*	ATGCAGCATCCCCATACACT	CACTCCCCAAACTCCAAACA	GgaAffx.12217.1.S1_at	1.89	188
10	Similar to lymphocyte binding protein 64	*CD180*	CTGGTACAGGCAGAATCTGG	CGCAGCACAAAACAACTAGG	Gga.7810.1.S1_at	1.94	158
11	LOC425969	*LOC425969*	GCAGTACATCCCACAGTGCT	CCCACTCTTTGCATCCCTTA	Gga.6572.1.A1_at	1.92	144
12	Homeobox, msh-like 2	*MSX2*	GCCCGTTGGACTCTATGCTA	CGGTTGGGTACTGCATTCTT	Gga.4977.1.S1_at	1.86	135
13	Protein-kinase, interferon-inducible RNA inhibitor	*PRKRIR*	GCTGTTCTTGGTGTGAAGTG	CAGTACTCCTGCCATGCTTG	GgaAffx.20873.1.S1_at	1.86	150
14	Rab22a	*Rab22a*	CTGTTGGCAGGGAGGTAGAG	CTTGAGCAGGCTGGTAGCAT	Gga.7554.1.S1_s_at	1.90	215
	Beta-Actin	*β*-Actin	CTGAACCCCAAAGCCAAC	CACCATCACCAGAGTCCATCAC		1.95	148
	Hypoxanthine phosphoribosyl -transferase	*HPRT*	TGGCGATGATGAACAAGGT	GCTACAATGTGGTGTCCTCCC		1.95	162

synthesis kit (VILO; Invitrogen, Karlsruhe, Germany) in a 20-μL reaction, according to the manufacturer's protocol. Two nanograms of cDNA were used per well as the template in a 15-μL reaction for fluorescence detection on a real-time PCR detection system (iCycler Multicolor; Bio-Rad, Hercules, CA), with a SYBR green master mix kit (QuantiTect; Qiagen). β-Actin and hypoxanthinephosphoribosyl-transferase (*HPRT*) were used as control genes for all reactions. Primers used for the analysis of the 14 candidate genes are shown in Table 1 and were validated through gel electrophoresis and automated sequencing. Primer efficiency (*E*) was determined from the slope of the curve generated through a cDNA dilution series, using the formula $E = 10^{(-1/\text{slope})}$ (Table 1).[32] Validation of expression data, by semiquantitative real-time RT-PCR, was undertaken by using (1) ACL samples processed (double amplified) and analyzed by microarray ($n = 3$ per experimental condition) and (2) independent ACL samples processed (double amplified) but not analyzed by microarray ($n = 3$ per experimental condition). Analysis of the 14 candidate genes by semiquantitative real-time RT-PCR was also performed within whole retinal (WR) samples taken from the left eye of chicks treated for 24 hours with either plus ($n = 5$) or minus ($n = 5$) lenses.

Pathway Analysis

Microarray data obtained from GC-RMA normalization were analyzed (Pathways Analysis System 5.0; Ingenuity Systems, Redwood City, CA), with chicken annotations converted into human orthologues for analysis.

Statistics

All data were originally compiled on a spreadsheet (Excel; Microsoft, Redmond, WA), and statistical calculations were performed (JMP 5.1 software package; SAS Institute GmbH, Munich, Germany). As is described in detail elsewhere,[9] the mean cycle threshold (C_t) value for each gene under each experimental condition was transformed into a mean normalized expression (MNE) value for statistical analysis, with HPRT and β-actin acting as housekeeping genes. All statistical comparisons of changes in RNA transcript expression levels between lens-treated animals and control groups for RT-PCR reactions were performed through analysis of variance (ANOVA) testing, with post hoc analysis using an unpaired Student's *t*-test. The genes were identified as differentially expressed if they showed a change of ≥ 1.5 with $P \leq 0.05$. The change ratio was calculated by dividing the experimental value (lens-treated) by the control value (age-matched untreated control). In cases in which this number was less than 1, the (negative) reciprocal is listed. A change of $+1$ or -1 indicates no change, whereas a change of 2 equals a doubling in product and a change of -2 equals a halving in transcript abundance.

Results

Microarray Analysis

Using the GC-RMA (GC-robust multiarray averaging) normalization methodology and a significance criterion of $P \leq 0.05$ and a change of ≥ 1.5-fold, we identified 128 differentially expressed genes by microarray analysis, within the ACL after 24 hours of minus lens treatment, compared with control values (Supplementary Table S1). This differential expression consisted of 63 upregulated and 65 downregulated genes, with changes ranging from +8.0- to -27.4-fold. Within the ACL of plus lens–treated eyes, 58 differentially expressed genes were observed after 24 hours of treatment (Supplementary Table S2). This group comprised 30 upregulated and 28 downregulated genes, with changes ranging from +7.7- to −5.7-fold. Most observed changes in gene expression (164 genes) were unique to either plus- or minus lens treatment, with only 11 genes showing a differential response to both treatments. When comparing minus lens– and plus lens–treated eyes, only 37 significant changes were detected, which consisted of 19 upregulated and 18 downregulated genes (Supplementary Table S3).

Microarray Validation

From the list of differentially expressed genes, generated by using a GC-RMA normalization method, 14 candidate genes were chosen for further analysis by real-time RT-PCR, based on previously defined roles within the body; pathway analysis, abundance in the ACL; and an appreciably large change ratio and/or probability. In general, the results obtained from microarray and real-time RT-PCR technologies correlated highly ($y = 0.85x + 1.32$, $r^2 = 0.49$, $P < 0.001$), with the exclusion of *ChEST49o10*, which was >3 SD outside the mean. All 14 candidate genes, whether differentially expressed in plus or minus tissue, were analyzed in both treatment groups via real-time RT-PCR.

Validation of Gene Expression Data in Microdissected ACL Samples. It was possible to validate eight of nine genes indicated to be differentially expressed in the minus lens–treated eyes (Fig. 2): validated genes included angiopoietin 2 (*ANGPT2*), *ChEST267a2*, *ChEST49o10*, D4, zinc and double PHD fingers, family 3 (*DPF3*), guanine nucleotide binding protein, gamma 13 (*GNG13*), glial cell line–derived neurotrophic factor family receptor alpha 1 (*GFRA1*), CD180 antigen (*CD180*), and *LOC425969*, while the nonvalidated genes included zinc finger DHHC domain-containing protein 14 (*DHHC14*). In plus lens–treated samples (Fig. 3), it was possible to validate four of eight genes indicated to be differentially expressed, including the validated genes *GFRA1*, general transcription factor IIH, polypeptide 5 (*GTF2H5*), *LOC425969*, and *Rab22a*, while those genes which were not validated by RT-PCR included cytochrome P450, family 26, subfamily a, polypeptide 1 (*CYP26A1*), *DHHC14*, Msh homeobox 2 (*MSX2*), protein-kinase, interferon-inducible double-stranded RNA dependent inhibitor (*PRKRIR*)) from the double amplified microdissected ACL samples. We also confirmed that there was no change in the expression of the remaining five candidate genes investigated in the minus lens–treated eyes (Table 2) and in four of five of the candidate genes in the plus lens–treated samples (Table 3), with the exception of the cDNA clone *ChEST49o10*, which showed a differential expression via PCR ($P = 0.01$) that was not observed by gene microarray ($P = 0.15$). In general, 75% (13/14 in the minus lens–treated group, 8 of 14 in the plus lens–treated group) of the investigated changes in gene expression were independently validated by semiquantitative RT-PCR, which included those genes indicated by microarray analysis not to display any change in expression level in response to plus or minus lens wear.

Comparison of Gene Expression Levels between the Whole Retina and the Amacrine Cell Layer. The expression levels of the candidate genes were measured within the whole retina to determine whether the observed changes were or were not confined to the ACL. We observed only two significant changes in transcript levels within the whole retina of the minus lens–treated eyes (*DPF3* and *GNG13*; Table 2); no significant changes were observed within the whole retina of the plus lens–treated eyes (Table 3).

Pathway Analysis

Human orthologues of GC-RMA normalized data were further analyzed (Pathways Analysis Software; Ingenuity Systems). The functional interactions between proteins and molecules that are shown in the proposed networks are supported by published information that is associated by the program with known biological pathways. The software suggested five distinct gene interaction pathways within the ACL of the minus lens–treated eyes and two in the plus lens–treated eyes (Fig. 4, Supplementary Figs. S1–S6). The major pathway predicted for the plus lens–treated eyes, in which 11 of 35 genes were found to be differentially expressed, was further analyzed (Fig. 4, differentially expressed genes are displayed in black). Using real-time RT-PCR, we investigated 5 of these 11 differentially expressed genes and validated the differential expression of *Rab22a*, *Egr-1*, and *GTF2H5*.

Discussion

Gene microarray analysis of LCM tissue detected 186 differentially expressed genes within the ACL of the chick retina in

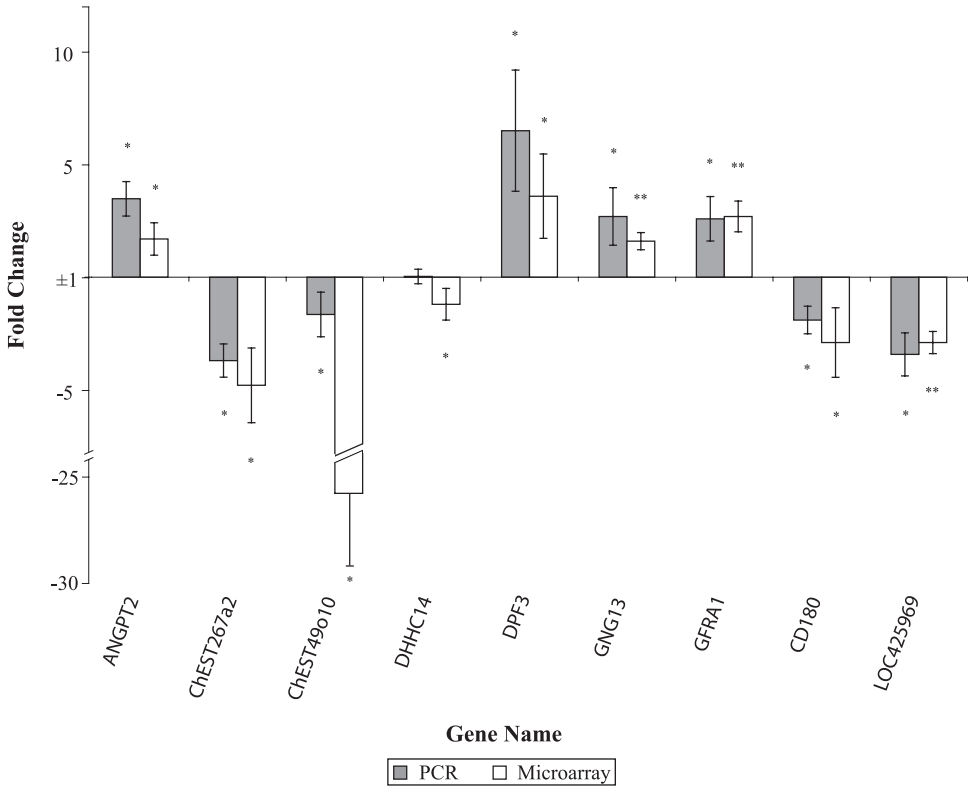

FIGURE 2. Candidate gene transcript levels in the ACL of minus lens–treated eyes, as detected by microarray analysis and real-time RT-PCR. Changes in gene expression are expressed as ratios ± SD. $^{*}P < 0.05$, $^{**}P < 0.01$.

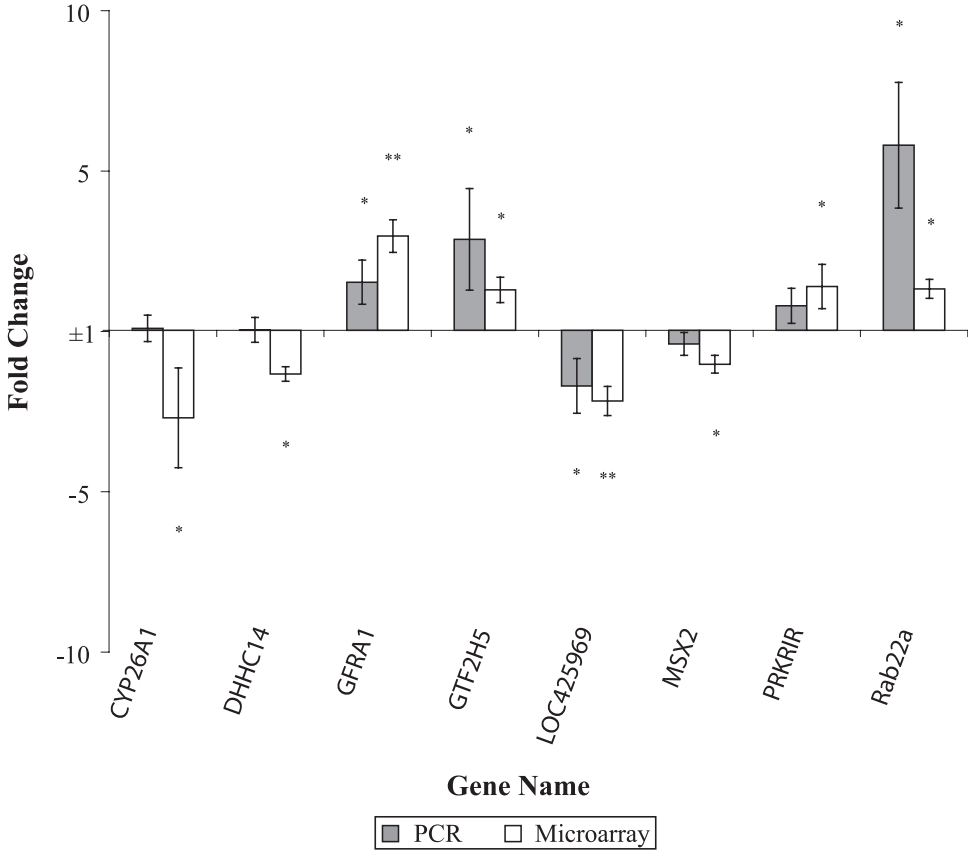

FIGURE 3. Candidate gene transcript levels in the ACL of plus lens–treated eyes, as detected by microarray analysis and real-time RT-PCR. Changes in gene expression are presented as ratios ± SD. $^{*}P < 0.05$, $^{**}P < 0.01$.

TABLE 2. Validation of Candidate Genes from Minus Lens–Treated Eyes, According to Real-Time RT-PCR

Gene No.	Gene Name	Probe ID	FC-Chip	*P*	FC-PCR	*P*	FC-WR	*P*
1	*ANGPT2*	Gga.3259.1.S1_at	2.7	**0.02**	4.5	**0.01**	−1.2	0.71
2	*ChEST267a2*	Gga.10694.1.S1_at	−5.8	**0.002**	−4.7	**0.05**	1.0	0.83
3	*ChEST49o10*	Gga.13753.1.S1_at	−27.4	**0.01**	−2.7	**0.03**	1.0	0.90
4	*CYP26A1*	Gga.331.1.S1_at	−3.1	0.06	1.6	0.48	−1.2	0.62
5	*DHHC14*	GgaAffx.21352.1.S1_at	−2.2	**0.03**	1.0	0.98	1.6	0.58
6	*DPF3*	Gga.46.1.S1_a_at	4.6	**0.009**	7.5	**0.02**	2.8	**0.03**
7	*GNG13*	Gga.10842.1.S1_at	2.6	**0.0002**	3.7	**0.03**	1.3	**0.02**
8	*GFRA1*	Gga.588.1.S1_at	3.7	**0.0009**	3.6	**0.03**	1.8	0.55
9	*GTF2H5*	GgaAffx.12217.1.S1_at	1.1	0.96	1.8	0.08	1.6	0.87
10	*CD180*	Gga.7810.1.S1_at	−3.9	**0.007**	−2.9	**0.04**	−1.2	0.17
11	*LOC425969*	Gga.6572.1.A1_at	−3.9	**0.0001**	−4.4	**0.02**	−2.8	0.36
12	*MSX2*	Gga.4977.1.S1_at	−1.5	0.7	1.0	0.98	−2.6	0.13
13	*PRKRIR*	GgaAffx.20873.1.S1_at	1.0	0.96	1.2	0.88	1.0	0.97
14	*Rab22a*	Gga.7554.1.S1_s_at	2.0	0.35	10.0	0.16	−1.2	0.53

Changes in gene expression are represented as the ratio of change, with a change of 1 equaling no change in gene expression and a change of 2 equalling a doubling in product. Minus values represent a reduction in gene expression. Probability values in bold represent statistically significant changes in RNA transcript levels ($P \leq 0.05$). FC, change ratio (*x*-fold); Chip, expression of candidate genes on the Affymetrix chips ($n = 3$, per experimental condition); PCR, PCR results from double-amplified LCM tissue processed for microarray analysis ($n = 6$, per experimental condition); WR, PCR results from whole retinal samples ($n = 5$, per experimental condition).

response to 24 hours of visual manipulation with spectacle lenses, with a larger number of changes observed in response to enhanced ocular growth (128 genes, minus lens wear), as opposed to growth suppression (58 genes, plus lens wear). In comparison to previous studies within the field, the magnitude of changes observed in this study was, in general, larger, with greater than 30% of differentially expressed genes showing a twofold or greater modulation in expression. This larger magnitude most likely represents a reduction in both noise and masking of transcript levels due to the more homogenous tissue sample analyzed presently. Only 11 genes were differentially expressed under both experimental conditions; the expression of only one (clone *ChEST927g14*) was dependent on the sign of focus. These results suggest that different retinal pathways are involved in plus and minus lens compensation, at least after 1 day of treatment. Most changes observed by microarray analysis should represent differential gene expression within retinal amacrine cells. Nevertheless, this fundal layer also contains the cell bodies of displaced bipolar and ganglion cells, as well as the processes of bipolar cells and Müller cells.

Independent Validation of Microarray Analysis

Validation of microarray data was undertaken using independent mRNA quantification techniques (real-time RT-PCR), with validation taken as a change >1.5-fold and $P < 0.05$. In general, the results from microarray and real-time RT-PCR technologies correlated highly, with 75% of the investigated genes independently validated, including those indicated by microarray analysis to have shown no change in expression level. The inability, however, to correlate changes in 25% of our investigated genes emphasizes the need for caution in interpreting gene expression data and may result from several issues, including the existence of nonspecific or alternative transcripts that cross-hybridize with the microarray probes, the existence of multiple isoforms of the gene differentially detected by microarray analysis and RT-PCR, and differences in normalization methodology between PCR and microarray analysis.

Pathway Analysis

Analysis of microarray data (Pathway Analysis; Ingenuity Systems) suggested five distinct pathways within the ACL of the

TABLE 3. Validation of Candidate Genes, from Plus Lens–Treated Eyes, According to Real-Time RT-PCR

Gene No.	Gene Name	Probe ID	FC-Chip	*P*	FC-PCR	*P*	FC-WR	*P*
1	*ANGPT2*	Gga.3259.1.S1_at	1.4	0.38	1.3	0.76	1.2	0.13
2	*ChEST267a2*	Gga.10694.1.S1_at	−1.6	0.27	1.4	0.21	1.6	0.07
3	*ChEST49o10*	Gga.13753.1.S1_at	−5.1	0.15	−5.1	**0.01**	1.3	0.32
4	*CYP26A1*	Gga.331.1.S1_at	−3.6	**0.03**	1.1	0.94	1.0	0.98
5	*DHHC14*	GgaAffx.21352.1.S1_at	−2.3	**0.03**	1.0	0.98	1.0	0.94
6	*DPF3*	Gga.46.1.S1_a_at	2.7	0.051	−4.3	0.70	1.7	0.44
7	*GNG13*	Gga.10842.1.S1_at	1.4	0.051	1.5	0.80	1.3	0.22
8	*GFRA1*	Gga.588.1.S1_at	3.8	**0.0007**	2.4	**0.04**	1.1	0.92
9	*GTF2H5*	GgaAffx.12217.1.S1_at	2.2	**0.03**	3.7	**0.03**	1.4	0.58
10	*CD180*	Gga.7810.1.S1_at	1.0	0.99	1.7	0.14	1.0	0.79
11	*LOC425969*	Gga.6572.1.A1_at	−3.1	**0.0002**	−2.7	**0.01**	−1.8	0.56
12	*MSX2*	Gga.4977.1.S1_at	−2.0	**0.014**	−1.4	0.72	−1.5	0.36
13	*PRKRIR*	GgaAffx.20873.1.S1_at	2.3	**0.02**	1.7	0.32	−1.2	0.43
14	*Rab22a*	Gga.7554.1.S1_s_at	2.2	**0.004**	6.5	**0.03**	−1.7	0.11

Changes in gene expression and explanation of column headings are as defined in Table 2. Probability values in bold represent statistically significant changes in RNA transcript levels ($P \leq 0.05$).

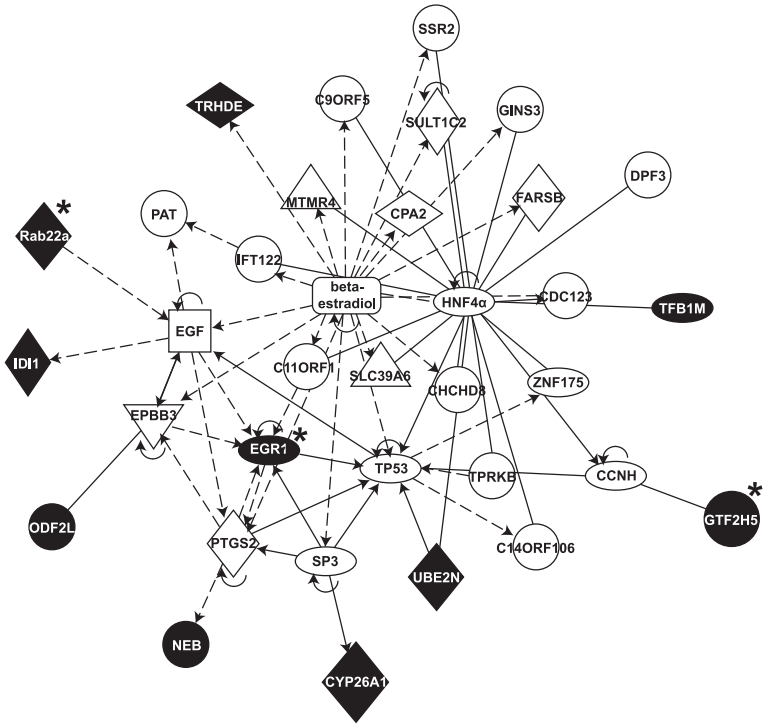

FIGURE 4. Analysis of gene interactions with pathway identity from GC-RMA normalized data for plus lens–treated ACL samples. *Filled symbols*: genes detected by microarray analysis to be differentially expressed; *asterisks*: genes that were independently validated by RT-PCR.

minus lens–treated samples and three in the plus lens–treated samples. These pathways are based on known human gene interactions, primarily within nonocular tissues. Detailed investigation of the major pathway predicted for the plus lens–treated samples, in which 11 of 35 genes were found to be differentially expressed (5 of which were investigated further), validated three of five changes (*Egr-1*, *GTF2H5*, and *Rab22a*). This predicted pathway, which warrants further investigation, was broadly defined as relating to cell signaling, development, and assembly. Key peptides within this predicted pathway included Egr-1, already postulated to play a key role in the regulation of ocular growth; β-estradiol; and hepatocyte nuclear factor 4, alpha (HNF4α). β-Estradiol is a steroid hormone synthesized mainly within the ovaries and to a lesser extent within peripheral tissues, including the retina. β-Estradiol appears to have neurotrophic and neuroprotective properties, increasing viability, survival, and differentiation of primary neurons in culture, and protecting retinal neurons against insults such as light damage and hydrogen peroxide treatment.[33,34] HNF4α encodes for a nuclear transcription factor that regulates the expression of numerous genes including members of the cytochrome P450 (CYP) family and HNF1.[35]

Gene Expression at the Whole Retina Level

Only two statistically significant changes, those of *DPF3* and *GNG13*, were observed within the whole retina of the eyes treated for 24 hours with minus lenses. No differential expression in transcript levels was observed in the whole retina of the plus lens–treated eyes. These findings support the hypothesis that changes in gene expression within the whole retina mask more specific changes occurring within the ACL. It should be noted though that RNA levels of the candidate genes, within the whole retina, were quite low and may therefore have reduced our ability to detect changes in their expression levels. In general, however, the lack of correlation between the changes seen within the ACL and whole retina emphasizes the possible loss of information, because of the heterogeneous nature of the retina, when investigating global changes in gene expression.

Comparison with Other Profiling Studies

A comparison of our current GC-RMA normalized microarray data, for both the plus- and minus lens–treated animals, against similar genetic studies in the field, indicated limited overlap in gene lists. The reduced overlap with previous microarray findings was, to some extent, expected, as these studies focused on changes in gene expression across the whole retina, or in some cases retina-RPE, or the retina-RPE-choroid. In contrast, we report in this study on the differential regulation of gene expression within a specific fundus layer of the eye, thereby significantly reducing the subtypes of ocular cells sampled compared with previous microarray studies.

A small number of genes, reported previously to be differentially expressed in response to visual manipulation, appeared on our current GC-RMA list. Comparisons with the study of McGlinn et al.,[7] who investigated changes in gene expression within a retinal-RPE tissue mix after 6 hours and 3 days of form deprivation (growth stimulant), indicated five common hits (*LOC420181*, *PRKRIR*, *SOUL*, *LOC419390*, and *LOC424393*). Comparisons with the study by Schippert et al.,[9] who investigated changes in gene expression within the retina of chicks treated for 1 day with plus lenses, indicated three common hits (Table 4; *LOC424393*, *ChEST914o3*, and *Egr-1*). They found the expression of *Egr-1* to be lower in the whole retina (−2.6-fold), with a similar finding observed in the ACL (−2.1-fold) in the present study. As they discussed, the unexpected downregulation in *Egr-1* expression suggests that the mRNA levels of this transcriptional regulator are upregulated in the short term (1–4 hours) by exposure to myopic defocus,[36] but appear to be downregulated in response to longer periods (24 hours) of positive lens wear. Further studies are necessary to determine the time kinetics of changes in *Egr-1* mRNA content in response to plus lens treatment.

No overlap was observed between our current findings and the other three major profiling studies.[8,10,11] This general lack of overlap may be due to several key differences among the studies, including the type of ocular tissue analyzed, the length and choice of treatment regimens, the type and age of gene

TABLE 4. Comparison of Current GC-RMA Normalized Microarry Data with Previous Microarray Studies in the Field

		Current Data			Current Data			McGlinn et al.		
Probe ID	Name	Treatment	Change Ratio	*P*	Treatment	Change Ratio	*P*	Treatment	Change Ratio	*P*
GgaAffx.24735.1.S1_at	LOC420181	Minus lens	2.0	0.005	Plus lens			FDM, 3 days	1.4	
GgaAffx.20873.1.S1_at	PRKRIR	Minus lens			Plus lens	2.3	0.024	FDM, 3 days	1.3	
Gga.1806.1.S1_at	SOUL	Minus lens	2.2	0.010	Plus lens			FDM, 3 days	1.3	
Gga.9574.1.S1_at	LOC419390	Minus lens			Plus lens	1.9	0.020	FDM, 3 days	1.2	
Gga.8944.3.S1_s_at	LOC424393	Minus lens	−1.6	0.027	Plus lens	−1.8	0.002	FDM, 3 days	1.2	

		Current Data			Current Data			Schippert et al.		
Probe ID	Name	Treatment	Change Ratio	*P*	Treatment	Change Ratio	*P*	Treatment	Change Ratio	*P*
Gga.8944.3.S1_s_at	LOC424393	Minus lens	−1.6	0.027	Plus lens	−1.8	0.002	Plus lens	2.2	<0.0001
GgaAffx.20379.1.S1_at	ChEST914o3	Minus lens			Plus lens	−1.8	0.045	Plus lens	−2.5	0.008
Gga.4922.1.S2_at	EGR-1	Minus lens			Plus lens	−2.1	0.045	Plus lens	−2.6	<0.0001

chip technology used, the species investigated, and the normalization methods used. Furthermore, the current literature suggests that reliable and reproducible detection of changes in gene expression by microarray analysis can be achieved for transcripts that show high abundance and relatively large changes in expression. However, the reliable measurement of genes of low abundance, which display small changes, is not as easily achievable.[37] As many of the gene expression changes according to microarray analysis in the field concern small changes in gene expression that show low abundance within the retina, this may further affect reproducibility between studies. Also, it has been noted that the reproducibility of microarray results is reduced if different array platforms are used, as opposed to comparisons between studies using similar platforms, in part because of identification of different splice variants of specific transcripts and differences in the amount and location of unwanted cross-hybridizations.[37]

The Expression of Known Markers of Ocular Growth

Several genes that have been postulated to play a role in the regulation of ocular growth also showed small but significant changes in expression, as assessed by microarray analysis. RNA levels of pre-pro glucagon, a known inhibitor of experimental eye growth,[15–16,38] showed a significant downregulation in response to minus lens wear, compared with those values seen within the ACL of the plus lens–treated eyes ($P = 0.04$). Cytochrome-*c* oxidase, subunit 1 mRNA levels have been shown by Feldkaemper et al.[23] to be significantly upregulated in the retina in response to 1 day of plus lens wear. Analysis of our current data indicates that the expression of cytochrome-*c* oxidase, subunit 6, isoform 1 and cytochrome-*c* oxidase assembly protein was significantly upregulated in response to 24 hours of minus lens wear ($P = 0.02$, $P = 0.04$, respectively). Unfortunately, no probe was present on the current microarray chips for cytochrome-*c* oxidase, subunit 1. We also observed a small but significant reduction in RNA levels of vasoactive intestinal peptide (*VIP*) receptor 1 within the ACL in response to plus lens wear in comparison to the minus lens–treated samples ($P = 0.03$). Previous studies have reported a significant upregulation in the expression of VIP RNA[11] and peptide levels[39] in primates after lid suturing, whereas microarray analysis of the retina/RPE after 3 days of deprivation myopia have indicated a significant downregulation in RNA levels of *VIP*.[7]

Several other molecules that have been proposed to play a role in the regulation of ocular growth were not observed to change in the present study, including members of the crystallin family (αA and αB, βA3, βA1, βB1, and βB2), bone morphogenetic protein 2, nitric oxide synthase, pax6, sox1/3, and sonic hedgehog. The overall lack of change in these molecules is most likely explained by differences in the time points measured, differences in the molecular level examined (e.g., peptide versus RNA), and differences in the treatment regimen used to elicit changes in their expression, as many of these changes have been reported in deprivation-myopia experiments, but not in lens paradigms. Most important, these molecules are probably not localized within the ACL. At least, no significant levels of crystallin, sox1, sonic hedgehog, and neuronal nitric oxide synthetase mRNA were detected in the present microarray analysis of the ACL.

The Detection of Novel Genes

The confirmed differential expression of several novel candidate genes could reflect a role for their peptide products in eye growth regulation in response to visual manipulation; however, they may also represent indirect responses to changes in global eye size and visual distortion induced by lens wear. Below, a brief description of the known biological role of each candidate gene for which differential expression was independently confirmed is given.

Angiopoietin 2. *ANGPT2* is a growth factor involved in physiological vasculogenesis and angiogenesis through binding to the Tie receptor family. It is also associated with pathologic neovascularization and diabetic macular edema and is known to be upregulated by hypoxia, retinal ischemia, and high glucose levels.[40–42] Its expression is also induced by various cytokines, including fibroblast growth factor (FGF)-2, and vascular endothelial growth factor (VEGF),[40,41] both of which have been postulated to play a role in the regulation of ocular growth (Nguyen KT, et al. *IOVS* 2009;50:ARVO E-Abstract 3840).[43]

D4, Zinc, and Double PHD Fingers, Family 3. Because of the presence of a double-paired finger motif, it is assumed that *DPF3* (*Cer-d4*) is involved in neurospecific transcriptional regulation via changes in the condensed/decondensed state of chromatin in the nucleus.[44] DPF3 expression is observed in many parts of the peripheral and central nervous system, but is concentrated highly within both the retina and cerebellum.[45]

Guanine Nucleotide Binding Protein (G Protein), Gamma 13. *GNG13* has been hypothesized to be involved in ON-bipolar cell signaling,[46] with recent evidence from animal

studies suggesting that bipolar cells may be critically involved in the regulation of ocular growth.[47–50]

Glial Cell Line–Derived Neurotrophic Factor (GDNF) Family Receptor Alpha 1. *GFRA1* is a glycosylphosphatidylinositol-linked cell surface receptor that binds, with high affinity, the potent neurotrophic factor GDNF, inducing activation of the RET protein-tyrosine kinase system. GDNF is critically involved in the development and maintenance of central and peripheral neurons, as well as the development of other organs, such as the kidney.[51,52]

General Transcription Factor IIH, Polypeptide 5. *GTF2H5* is essential for RNA polymerase II transcription and nucleotide excision repair, as part of a multicellular complex with transcription repair factor IIH (*TFIIH*).[53,54] Cells lacking GTF2H5 show reduced DNA repair activity, whereas yeast lacking this protein have been found to grow slowly and to be sensitive to UV radiation.[54]

CD180. Similar to lymphocyte-binding protein 64 this cell surface molecule belongs to the family of pathogen receptors (Toll-like receptors) that trigger innate immune responses, but are also involved in several other physiological functions including the regulation of retinal progenitor cell proliferation, RPE transmembrane signaling involved in photoreceptor disc shedding, establishing dorsal–ventral axis polarity, and synaptogenesis (for review, see Ref. 55).

Rab22a. This protein is a member of the Rab family of small GTPases, and is expressed ubiquitously in mammalian tissues. Rab proteins are involved in diverse functions associated with the control of intracellular membrane trafficking (for review, see Ref. 56).

***LOC425969*, *ChEST267a2*, and *ChEST49o10*.** No information is currently available with regard to the structure or function of the ESTs ChEST267a2 and ChEST49o10 or the predicted protein LOC425969.

Conclusions

We successfully removed the ACL by LCM and analyzed changes in gene expression by using microarray analysis, after plus (suppressed ocular growth) and minus (ocular growth stimulation) lens treatment. GC-RMA normalization showed 186 changes in gene expression within the ACL in response to lens treatment. Most of these changes seem to be confined to the cells of the ACL since they were not observed within the whole retina. Moreover, we hypothesize that different retinal pathways may be involved in plus and minus lens compensation since there was limited overlap in the genes regulated by both conditions. From the list of differentially expressed genes, we have identified and validated several novel genes that may form part of the growth regulatory system of the eye.

Acknowledgments

The authors thank Eva Burkhardt and Monika Schuetz (Institute for Medical Microbiology and Hygiene, University of Tübingen) for technical assistance with laser capture microdissection and Britta Baumann for technical assistance with PCR sequencing.

References

1. Morgan I, Rose K. How genetic is school myopia? *Prog Retin Eye Res.* 2005;24:1–38.
2. Saw SM, Gazzard G, Shih-Yen EC, Chua WH. Myopia and associated pathological complications. *Ophthalmic Physiol Opt.* 2005;25:381–391.
3. Wallman J, Turkel J, Trachtman J. Extreme myopia produced by modest change in early visual experience. *Science.* 1978;201:1249–1251.
4. Schaeffel F, Glasser A, Howland HC. Accommodation, refractive error and eye growth in chickens. *Vision Res.* 1988;28:639–657.
5. Wildsoet CF, Wallman J. Choroidal and scleral mechanisms of compensation for spectacle lenses in chicks. *Vision Res.* 1995;35:1175–1194.
6. Nickla DL, Wildsoet C, Wallman J. Compensation for spectacle lenses involves changes in proteoglycan synthesis in both the sclera and choroid. *Curr Eye Res.* 1997;16:320–326.
7. McGlinn AM, Baldwin DA, Tobias JW, Budak MT, Khurana TS, Stone RA. Form-deprivation myopia in chick induces limited changes in retinal gene expression. *Invest Ophthalmol Vis Sci.* 2007;48:3430–3436.
8. Rada JA, Wiechmann AF. Ocular expression of avian thymic hormone: changes during the recovery from induced myopia. *Mol Vis.* 2009;15:778–792.
9. Schippert R, Schaeffel F, Feldkaemper MP. Microarray analysis of retinal gene expression in chicks during imposed myopic defocus. *Mol Vis.* 2008;14:1589–1599.
10. Brand C, Schaeffel F, Feldkaemper MP. A microarray analysis of retinal transcripts that are controlled by image contrast in mice. *Mol Vis.* 2007;13:920–932.
11. Tkatchenko AV, Walsh PA, Tkatchenko TV, Gustincich S, Raviola E. Form deprivation modulates retinal neurogenesis in primate experimental myopia. *Proc Natl Acad Sci U S A.* 2006;103:4681–4686.
12. Lam TC, Li KK, Lo SC, Guggenheim JA, To CH. A chick retinal proteome database and differential retinal protein expressions during early ocular development. *J Proteome Res.* 2006;5:771–784.
13. Bertrand E, Fritsch C, Diether S, et al. Identification of apolipoprotein A-I as a "STOP" signal for myopia. *Mol Cell Proteomics.* 2006;5:2158–2166.
14. Fischer AJ, McGuire JJ, Schaeffel F, Stell WK. Light- and focus-dependent expression of the transcription factor ZENK in the chick retina. *Nat Neurosci.* 1999;2:706–712.
15. Feldkaemper MP, Schaeffel F. Evidence for a potential role of glucagon during eye growth regulation in chicks. *Vis Neurosci.* 2002;19:755–766.
16. Vessey KA, Lencses KA, Rushforth DA, Hruby VJ, Stell WK. Glucagon receptor agonists and antagonists affect the growth of the chick eye: a role for glucagonergic regulation of emmetropization? *Invest Ophthalmol Vis Sci.* 2005;46:3922–3931.
17. Stone RA, Lin T, Laties AM, Iuvone PM. Retinal dopamine and form-deprivation myopia. *Proc Natl Acad Sci U S A.* 1989;86:704–706.
18. Rohrer B, Spira AW, Stell WK. Apomorphine blocks form-deprivation myopia in chickens by a dopamine D2-receptor mechanism acting in retina or pigmented epithelium. *Vis Neurosci.* 1993;10:447–453.
19. Hammond CJ, Andrew T, Mak YT, Spector TD. A susceptibility locus for myopia in the normal population is linked to the PAX6 gene region on chromosome 11: a genomewide scan of dizygotic twins. *Am J Hum Genet.* 2004;75:294–304.
20. Ashby RS, Megaw PL, Morgan IG. Changes in the expression of Pax6 RNA transcripts in the retina during periods of altered ocular growth in chickens. *Exp Eye Res.* 2009;89:392–397.
21. Fischer AJ, Wallman J, Mertz JR, Stell WK. Localization of retinoid binding proteins, retinoid receptors, and retinaldehyde dehydrogenase in the chick eye. *J Neurocytol.* 1999;28:597–609.
22. Bitzer M, Feldkaemper M, Schaeffel F. Visually induced changes in components of the retinoic acid system in fundal layers of the chick. *Exp Eye Res.* 2000;70:97–106.
23. Feldkaemper MP, Wang HY, Schaeffel F. Changes in retinal and choroidal gene expression during development of refractive errors in chicks. *Invest Ophthalmol Vis Sci.* 2000;41:1623–1628.
24. Fukuda M, Kuwayama Y, Shiosaka S, et al. Localization of vasoactive intestinal polypeptide and neurotensin immunoreactivities in the avian retina. *Curr Eye Res.* 1981;1:115–118.
25. Seltner RL, Stell WK. The effect of vasoactive intestinal peptide on development of form deprivation myopia in the chick: a pharmacological and immunocytochemical study. *Vision Res.* 1995;35:1265–1270.

26. Ashby R, McCarthy CS, Maleszka R, Megaw P, Morgan IG. A muscarinic cholinergic antagonist and a dopamine agonist rapidly increase ZENK mRNA expression in the form-deprived chicken retina. *Exp Eye Res.* 2007;85:15–22.
27. Stone RA, Lin T, Laties AM. Muscarinic antagonist effects on experimental chick myopia. *Exp Eye Res.* 1991;52:755–758.
28. McBrien NA, Moghaddam HO, Reeder AP. Atropine reduces experimental myopia and eye enlargement via a nonaccommodative mechanism. *Invest Ophthalmol Vis Sci.* 1993;34:205–215.
29. Wildsoet CF, Pettigrew JD. Kainic acid-induced eye enlargement in chickens: differential effects on anterior and posterior segments. *Invest Ophthalmol Vis Sci.* 1988;29:311–319.
30. Fischer AJ, Seltner RL, Stell WK. N-methyl-D-aspartate-induced excitotoxicity causes myopia in hatched chicks. *Can J Ophthalmol.* 1997;32:373–377.
31. Fischer AJ, Morgan IG, Stell WK. Colchicine causes excessive ocular growth and myopia in chicks. *Vision Res.* 1999;39:685–697.
32. Pfaffl MW. A new mathematical model for relative quantification in real-time RT-PCR. *Nucleic Acids Res.* 2001;29:e45.
33. Yu X, Rajala RV, McGinnis JF, et al. Involvement of insulin/phosphoinositide 3-kinase/Akt signal pathway in 17 beta-estradiol-mediated neuroprotection. *J Biol Chem.* 2004;279:13086–13094.
34. Lorenzo A, Diaz H, Carrer H, Caceres A. Amygdala neurons in vitro: neurite growth and effects of estradiol. *J Neurosci Res.* 1992;33:418–435.
35. Tirona RG, Lee W, Leake BF, et al. The orphan nuclear receptor HNF4alpha determines PXR- and CAR-mediated xenobiotic induction of CYP3A4. *Nat Med.* 2003;9:220–224.
36. Simon P, Feldkaemper M, Bitzer M, Ohngemach S, Schaeffel F. Early transcriptional changes of retinal and choroidal TGFbeta-2, RALDH-2, and ZENK following imposed positive and negative defocus in chickens. *Mol Vis.* 2004;10:588–597.
37. Draghici S, Khatri P, Eklund AC, Szallasi Z. Reliability and reproducibility issues in DNA microarray measurements. *Trends Genet.* 2006;22:101–109.
38. Vessey KA, Rushforth DA, Stell WK. Glucagon- and secretin-related peptides differentially alter ocular growth and the development of form-deprivation myopia in chicks. *Invest Ophthalmol Vis Sci.* 2005;46:3932–3942.
39. Stone RA, Laties AM, Raviola E, Wiesel TN. Increase in retinal vasoactive intestinal polypeptide after eyelid fusion in primates. *Proc Natl Acad Sci U S A.* 1988;85:257–260.
40. Mandriota SJ, Pepper MS. Regulation of angiopoietin-2 mRNA levels in bovine microvascular endothelial cells by cytokines and hypoxia. *Circ Res.* 1998;83:852–859.
41. Oh H, Takagi H, Suzuma K, Otani A, Matsumura M, Honda Y. Hypoxia and vascular endothelial growth factor selectively up-regulate angiopoietin-2 in bovine microvascular endothelial cells. *J Biol Chem.* 1999;274:15732–15739.
42. Sivakumar V, Zhang Y, Ling EA, Foulds WS, Kaur C. Insulin-like growth factors, angiopoietin-2, and pigment epithelium-derived growth factor in the hypoxic retina. *J Neurosci Res.* 2008;86:702–711.
43. Rohrer B, Stell WK. Basic fibroblast growth factor (bFGF) and transforming growth factor beta (TGF-beta) act as stop and go signals to modulate postnatal ocular growth in the chick. *Exp Eye Res.* 1994;58:553–561.
44. Aasland R, Gibson TJ, Stewart AF. The PHD finger: implications for chromatin-mediated transcriptional regulation. *Trends Biochem Sci.* 1995;20:56–59.
45. Ninkina NN, Mertsalov IB, Kulikova DA, et al. Cerd4, third member of the d4 gene family: expression and organization of genomic locus. *Mamm Genome.* 2001;12:862–866.
46. Huang L, Max M, Margolskee RF, Su H, Masland RH, Euler T. G protein subunit G gamma 13 is coexpressed with G alpha o, G beta 3, and G beta 4 in retinal ON bipolar cells. *J Comp Neurol.* 2003;455:1–10.
47. Crewther DP, Crewther SG. Pharmacological modification of eye growth in normally reared and visually deprived chicks. *Curr Eye Res.* 1990;9:733–740.
48. Zhong X, Ge J, Smith EL 3rd, Stell WK. Image defocus modulates activity of bipolar and amacrine cells in macaque retina. *Invest Ophthalmol Vis Sci.* 2004;45:2065–2074.
49. Chen JC, Brown B, Schmid KL. Slow flash multifocal electroretinogram in myopia. *Vision Res.* 2006;46:2869–2876.
50. Crewther DP, Crewther SG, Xie RZ. Changes in eye growth produced by drugs which affect retinal ON or OFF responses to light. *J Ocul Pharmacol Ther.* 1996;12:193–208.
51. Moore MW, Klein RD, Farinas I, et al. Renal and neuronal abnormalities in mice lacking GDNF. *Nature.* 1996;382:76–79.
52. Enomoto H, Araki T, Jackman A, et al. GFR alpha1-deficient mice have deficits in the enteric nervous system and kidneys. *Neuron.* 1998;21:317–324.
53. Giglia-Mari G, Miquel C, Theil AF, et al. Dynamic interaction of TTDA with TFIIH is stabilized by nucleotide excision repair in living cells. *PLoS Biol.* 2006;4:e156.
54. Ranish JA, Hahn S, Lu Y, et al. Identification of TFB5, a new component of general transcription and DNA repair factor IIH. *Nat Genet.* 2004;36:707–713.
55. Shechter R, Ronen A, Rolls A, et al. Toll-like receptor 4 restricts retinal progenitor cell proliferation. *J Cell Biol.* 2008;183:393–400.
56. Kauppi M, Simonsen A, Bremnes B, et al. The small GTPase Rab22 interacts with EEA1 and controls endosomal membrane trafficking. *J Cell Sci.* 2002;115:899–911.